Amount of Free Carbon in Spheroidal Graphite Iron Castings with Different Modulus

T. Kotani
Matsue Division, Yanmar Casting Technology Co., Ltd., Matsue, Shimane, Japan

K. Edane
Tsuchiyoshi Industry Co., Ltd., Ochi-gun, Shimane, Japan

H. Kambayashi
Tsuchiyoshi Industry Co., Ltd., Nishi-ku, Hiroshima, Japan

K. Iwakado
Chiyoda Plant, Ota Chuzosho Co., Ltd. Yamagata-gun, Hiroshima, Japan

H. Itofuji
Adstefan/Casting-Solution Center, University of Tohoku, Sendai, Miyagi, Japan

ABSTRACT

To clarify why shrinkage-free quality spheroidal graphite iron castings can be obtained without risers in the casting modulus (M) range >3.0 cm (1.2 in.) but not for M<3.0 cm (1.2 in.), free carbon as graphite precipitated until the end of solidification and was analyzed for test castings with M=0.5–5.0 cm (0.2–1.96 in.). Each casting was quenched in water after solidification. Samples were taken from the castings and their free carbon content was analyzed according to JIS G 1211-5(ISO/TR 10719). The amount of free carbon was almost the same for all of the castings. This is different from previously reported results, where the free-carbon value in castings with M<3.0 cm (1.2 in.) was less than that in castings with M>3.0 cm (1.2 in.). In this study, it is concluded that the amount of free carbon is a necessary but not a sufficient condition as a shrinkage countermeasure in castings. The precipitation timing and amount of free carbon with the progress of solidification may be related to shrinkage.

Keywords: free carbon, riser design, spheroidal graphite iron, shrinkage

INTRODUCTION

Graphite precipitation during solidification has a large influence on shrinkage in castings.[1] If expansion is effectively used, riser-less design is possible. In fact, many researchers had reported riser-less design using the modulus and shape factor of castings.[2-7] However, it is generally believed that riser-less design is not possible for castings with casting modulus (M=V/S, where V is the volume and S is the surface area) less than 2.5 cm (1 in.).

According to Goto et al.[7] and Chang,[6] this is the reason why the amount of graphite precipitation as free carbon is not sufficient for M<2.5 cm (1 in.) while it is saturated for M>2.5 cm (1 in.). In their studies, free carbon just after solidification was analyzed by converting two-dimensional (2D) morphological images to three-dimensional (3D) volumes, and then the volume was changed into a mass percent.

In this study, free carbon as graphite was extracted from samples that were quenched just after solidification, and it was directly analyzed by the infrared absorption method.

EXPERIMENTAL PROCEDURE

FOUNDRY EXPERIMENTS

First, a solidification curve for sample castings with M=0.5–5.0 cm (0.2–1.96 in.) was determined. The sizes and cast design of the sample castings are shown in Table 1 and Fig. 1, respectively.

Table 1. Sizes of Sample Castings with Different Modulus

M (cm)	Diameter × height (mm)
0.5	30 × 30
1.0	60 × 60
2.0	120 × 120
3.0	180 × 180
4.0	240 × 240
5.0	300 × 300

Molten iron was prepared using a 5 ton (4535.9 kg) high frequency induction furnace and was treated with 1.25 wt% Fe-Si-6.1mass%Mg and 0.4 wt% Fe-47mass%Si by the sandwich method during tapping. Steel scrap chips of 1.0 wt% was covered on the alloys.

Mg-treated molten iron was poured into a furan silica sand mold at about 1380C (2516F). Solidification curves of each sample casting were measured at the center as master curves for the following quenching experiment.

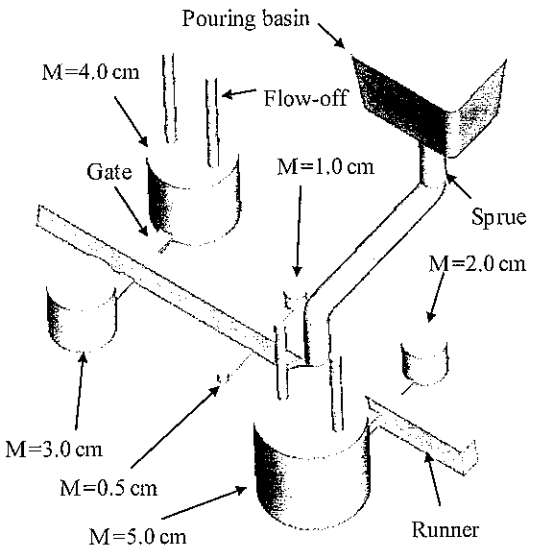

Molding flask size: 1800 mm × 1350 mm × 900 mm (height)

Fig. 1. Schematic shows the cast design for sample casting in the furan sand mold.

LABORATORY EXPERIMENTS

The sample castings were then quenched after solidification and the amount of free carbon was determined. Molten iron was prepared using a 30 kg (66 lb) high frequency induction furnace. The chemical composition was the same as the first melting in the foundry with the same raw materials and treated with the same alloys.

The samples that were analyzed for free carbon were quenched to maintain the conditions at the end of solidification. Therefore, the samples were small enough to quench. They were divided into two groups. One was the group with M=0.5–2.0 cm (0.2–0.8 in.). These samples were molded with furan silica sand and Mg-treated molten iron. Their solidification behavior was monitored with K-type thermocouples at the center of the samples. They were quenched in water at about 1100C (2012F). The other group was the group with M=3.0–5.0 cm (1.2–1.9 in.). As shown in Fig. 2, Mg-treated iron was poured into graphite crucibles and cooled in the control furnace, reproducing the solidification curves measured in the foundry. Monitoring and quenching were conducted using the same procedure described previously.

Analysis specimens of 10 × 10 × 1 mm^3 (0.0006 x 0.0006 x 0.00006 $in.^3$) were taken from the samples near the thermocouple using a microcutter; castings and their free carbon were analyzed according to JIS G1211-5 (ISO/TR 10719). The free carbon (i.e., graphite) was filtered out from the acid resolution liquid using a 0.3-μm glass-fiber filter. The total carbon was analyzed by the infrared absorption method (CS-LS600, Leco Corp.).

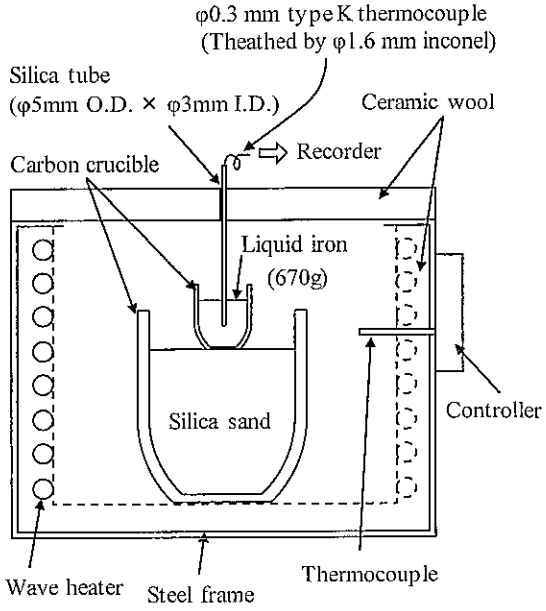

Fig. 2. Experimental apparatus for the laboratory experiments is shown.

RESULTS AND DISCUSSION

The chemical composition of Mg-treated molten iron in the foundry is given in Table 2. The solidification curves of sample castings measured in the foundry are shown in Fig. 3. Undercooling phenomena of the eutectic temperature were observed for sample castings with M<3.0 cm (1.2 in.). The eutectic temperatures of the samples with M=3.0–5.0 cm (1.2–1.9 in.) were almost the same.

Table 2. Chemical Composition in the Foundry Experiment (mass%)

C	Si	Mn	P	S	Mg
3.33	2.41	0.32	0.025	0.010	0.047

The chemical composition of Mg-treated molten iron in the laboratory experiment is shown in Table 3. The solidification curves of the sample castings measured in the laboratory are shown in Fig. 4. Figure 4 indicates that the solidification behavior shown in Fig. 3 is reproduced well, except at the early stage of the solidification curve. This is the reason why the sampling temperature in the laboratory was higher than that in the foundry.

The microstructures of the sample castings quenched in water after solidification are shown in Fig. 5. The microstructures were observed at a position near the thermocouple. Good morphology spheroidal graphite was

obtained, as shown in Fig. 5. There was a small amount of the ledeburite structure in the sample castings with M=3.0–5.0 cm (1.2–1.9 in.) but not in the samples with M=0.5–2.0 cm (0.2–0.8 in.). The existence of the ledeburite structure means that solidification was not complete when the sample castings were quenched. However, it is considered that the amount has almost no influence on the results of this study.

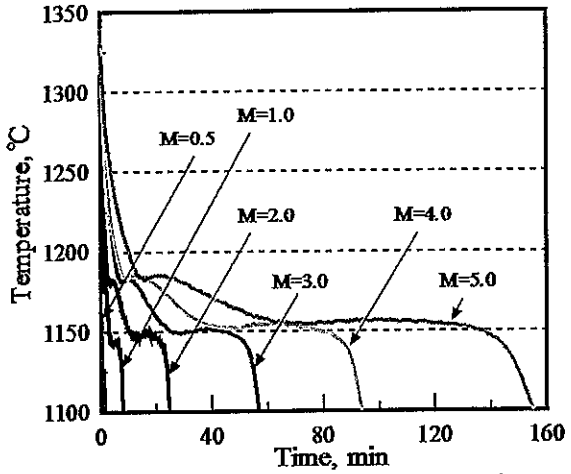

Fig. 3. Solidification curves for sample castings with M=0.5–5.0 cm (0.2–2 in.) in the foundry experiments are graphed.

Table 3. Chemical Compositions in the Laboratory Experiments (mass%)

Sample Casting M (cm)	C	Si	Mn	P	S	Mg
1.0 2.0 4.0	3.42	2.45	0.30	0.024	0.010	0.047
3.0	3.39	2.41	0.32	0.029	0.015	0.041
5.0	3.46	2.36	0.27	0.029	0.015	0.050
0.5	3.46	2.38	0.29	0.022	0.015	0.046

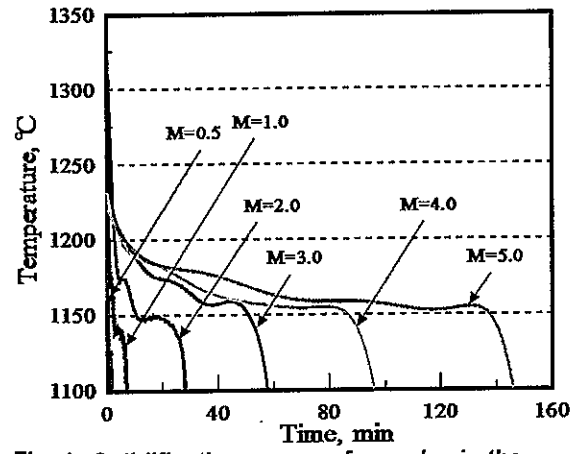

Fig. 4. Solidification curves of samples in the laboratory experiments are graphed.

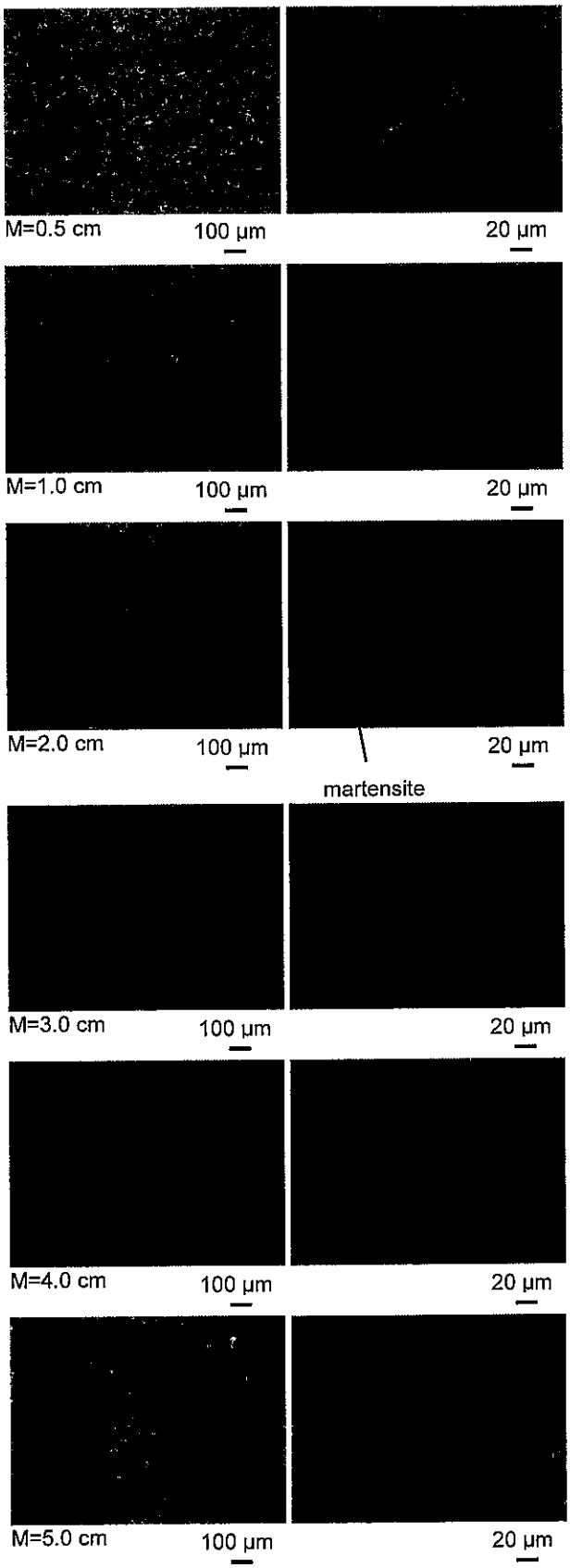

Fig. 5. Microstructures of sample castings quenched after solidification (5 mass% nital etch) are shown.

Because the chemical compositions of the sample castings in the laboratory are not the same, the analytical results are given as free carbon to total carbon percentage (called the free/total carbon ratio). The modulus was converted to solidification time according to the results of thermal analysis. The relationship between the free/total carbon ratio and the solidification time is shown in Fig. 6.

The free/total carbon ratio is almost the same for all of the sample castings. This is different from previously reported results, where the amount of graphite decreased because of hypersaturation of carbon in austenite when the solidification time was <20 min.[6,7] However, the graphite ratio was obtained by 2D morphological image analysis. This analysis is less accurate because the results depend on the polished condition of the sample and the detection limit.

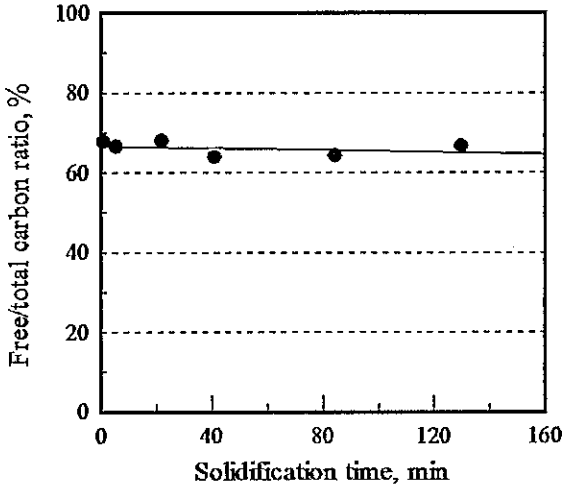

Fig. 6. Relationship between solidification time and free/total carbon ratio is graphed.

The validity of the test results was considered. According to Heine[8] and Hocheid et al.,[9] the carbon solubility in austenite is defined using Eqns. 1 and 2. Table 4 shows the calculated carbon solubility in austenite from Eqns. 1 and 2. The results of this study are also given in Table 4. If these equations are reasonable, the results of this study indicate that hypersaturation of carbon in austenite does not occur.

$C\gamma$ mass% = 2.1 – 0.217 Si ***Eqn. 1***[8]

$C\gamma$ mass% = 2.045 – 0.178 Si ***Eqn. 2***[9]

The Fe-C phase diagram for 2.5 mass% Si is shown in Fig. 7.[10] The results of this study are plotted and they are all in the austenite region.

Table 4. Calculated Carbon Solubility in Austenite for the Optional Silicon Content (Mass%)

Silicon		2.45	2.41	2.36	2.38
Carbon solubility in austenite	Eqn. 1 [8]	1.57	1.58	1.59	1.58
	Eqn. 2 [9]	1.61	1.62	1.62	1.62
	This study (Ave. n=2)	1.16	1.23	1.16	1.12

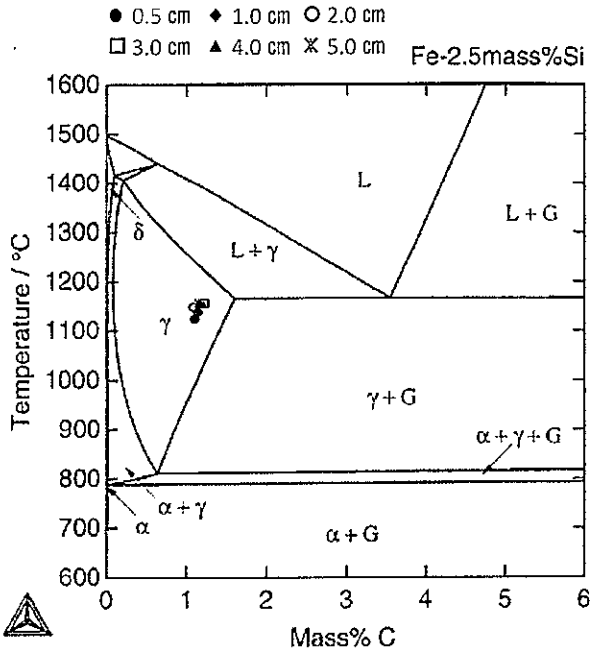

Fig. 7. Relationship between carbon solubility and eutectic temperature on the Fe-C-2.5%Si phase diagram.

If the results in this study are plotted on the Fe-C-2.4mass%Si phase diagram proposed by Hanemann,[11] they are almost on the limit of carbon saturation in austenite, as shown in Fig. 8. An enlargement of the Fe-C-2.5mass%Si phase diagram in Fig. 7 is shown in Fig. 8 to clearly show the results of this study.

As mentioned previously, it is clear that the amount of free carbon as graphite, which is related to shrinkage formation, is almost the same for the castings even though the modulus is greatly different. Hypersaturation of carbon in austenite did not occur. However, when the spheroidal graphite iron casting has M<3.0 cm (1.2 in.), there is a high probability of shrinkage defects occurring. Therefore, it is considered that the amount of free carbon is a necessary but not sufficient condition as a shrinkage countermeasure in castings. The precipitation timing and amount of free carbon during the solidification progress may be related to shrinkage.

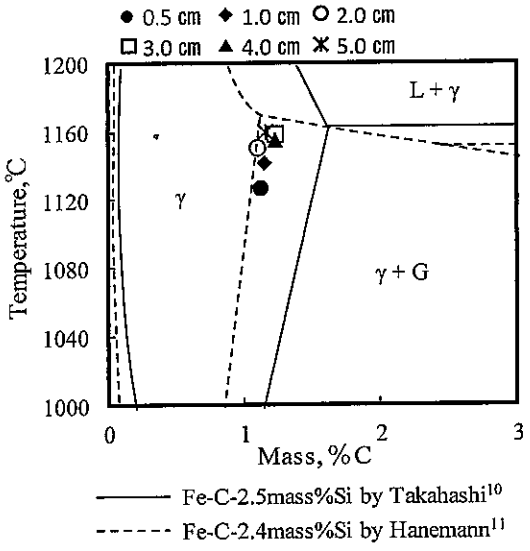

Fig. 8. Detailed Fe-C-Si phase diagram near the eutectic temperature is shown.

The amount of free carbon as graphite increases from the view point of nodule count when chillers are used and postinoculation is effectively conducted. It has been reported that the growth of graphite during solidification may depend on carbon diffusion in the austenite shell.[12,13] Because silicon mostly segregates in the austenite shell and gradually decreases with time, the growth of graphite may be influenced by change of the silicon density. Furthermore, software for producing the Fe-C-Si phase diagram will improve its accuracy and aid in the future development of spheroidal graphite iron castings.

CONCLUSIONS

Direct quantitative analysis according to JIS G1211-5 was used for castings with different modulus. The following conclusions can be drawn:

- The amount of free carbon was almost equal among all of the castings even though there was a large difference in their modulus values.
- The eutectic temperature was almost constant in the castings with M>3.0 cm (1.2 in.).
- The eutectic temperature decreased when the casting modulus decreased below 3.0 cm (1.2 in.).
- The amount of free carbon at the end of solidification was not a direct factor on shrinkage.

REFERENCES

1. Gough, M.J., Morgan, J., "Feeding Ductile Iron Castings-Some Recent Experiments," *American Foundry Society Transactions*, vol. 84, pp. 351-384 (1976).
2. Karsay, S.I., "Ductile Iron I-Production," *Quebec Iron and Titanium* (1976).
3. Karsay, S.I., "Ductile Iron III-Design of Gating System and Riser," *Quebec Iron and Titanium* (1981).
4. Taffazzoli, M., Kondic, V., "Making Sound Ductile Iron Castings without Risers," *Foundry Management and Technology*, vol. 104(12), pp. 86ff (1976).
5. Taffazzoli, M., Kondic, V., "Volume Contraction and Shrinkage Cavities Behavior in Ductile Iron Castings," *AFS International Cast Metals Journal*, vol. 2(12), pp. 41-47 (1977).
6. Chang, B., "The Riserless Design of Ductile Cast Iron," *Imono*, vol. 55(2), pp. 113-120 (1983).
7. Goto, A., Aizawa, T., Okada, S., "On the Amount of Graphite Formed during Freezing and Cooling in Spheroidal Graphite Cast Iron," *Imono*, vol. 50(6), pp. 345-349 (1978).
8. Heine, R.W., "The Carbon Equivalent Fe-C-Si Diagram and its Application to Cast Irons," *AFS Cast Metals Research Journal*, vol. 7, pp. 49-54 (1971).
9. Hocheid, B., Poupeau, P., "Diagrammes d'équilibre: Alliages ternaires" (10 juil, 1978).
10. Takahashi, T., Oikawa, K., "The Fe-C-Si System Ternary Calculation Phase Diagram," *Tohoku Industrial Technology Laboratory T/R*, vol. 23, pp. 192-197 (1999).
11. Hanemann, H., Jass, H., "Ueber das System Eisen-Eisensilizid FeSi-Graphit," *Giesserei*, vol. 25, pp. 293-299 (1938).
12. Wittmoser, A., "Zur Bildung des Kugelgraphits im Gusseisen," *Giesserei*, vol. 38, pp. 572-577 (1951).
13. Itofuji, H., "Study on Graphite Spheriodization in Cast Irons," Doctoral Thesis, Kyoto University (1993).